JTTEE5 18:411–420
DOI: 10.1007/s11666-009-9322-5
1059-9630/$19.00 © ASM International

Multiscale Model on Deposition Behavior of Agglomerate Metal Particles in a Low-Temperature High-Velocity Air Fuel Spraying Process

Xiaojing Yuan, Bailin Zha, Genliang Hou, Pingjun Hou, Li Jiang, and Hangong Wang

(Submitted September 12, 2008; in revised form February 17, 2009)

A multiscale model was constructed for agglomerate metal particle deposition in a low-temperature high-velocity air fuel (LTHVAF) thermal spraying process using finite element analysis (FEA) and smoothed particle hydrodynamics (SPH). Here, the agglomerate particle impact on the substrate is simplified to three states. Then, the corresponding model is selected. The simulated results show that the temperature and velocity of agglomerate particle can affect the effective temperature and plastic strain in the contact interface for increasing particle energy. At the microscale, the deformation of the deposited particle might coarsen the coating surface to the extent that the critical velocity of the metal particle would decrease. It indicates that the agglomerate particle might splash when it impacts on the substrate. The transient melting can be ascertained at an angle in an approach to the achievement of intermetallics combined with the modeling of the particle penetrating into the substrate. In this process, the effective strain of an agglomerate particle at the nanoscale is less than that at microscale, but the surface area ratio at nanoscale is large. The uncompacted state of the agglomerate particle can lead to a turbulent force when the agglomerate particle deposits on the substrate, which can reduce the penetration performance of the particle. This behavior can decrease the stress-strain of substrate and cause the cracked particle to sparkle.

Keywords agglomerate particle, deposition characteristics, numerical simulation, smooth particle hydrodynamics, thermal spray

1. Introduction

In the low-temperature high-velocity air fuel (LTHVAF) spraying process, a wide variety of phenomena are observed when particles with a velocity of approximately at 300 to 800 m/s impinge upon the solid substrate surface, which often relates to a supersonic impact (Ref 1-3). In related technical applications, agglomerate particles and aggregate particles can be accelerated by a supersonic gas flow emanating from a de Laval nozzle. Under impact conditions corresponding with the spray region, particles can form a strong bond with the substrate surface. This important phenomenon of particle deposition is strongly influenced by a collective interaction of the particles with the substrate.

Xiaojing Yuan, Bailin Zha, Pingjun Hou, Li Jiang, and **Hangong Wang**, Xi'an Research Institute of Hi-Tech, Hongqing Town, Xi'an, Shaanxi 710025, P.R. China; and **Genliang Hou**, Xi'an Research Institute of Hi-Tech, Hongqing Town, Xi'an, Shaanxi 710025, P.R. China and Materials Science and Engineering School, Xi'an Jiaotong University, Xi'an, Shaanxi 710049, P.R. China. Contact e-mail: yxj2003@263.net.

Recently, work concentrated on the deposition mechanism of aggregate particles in order to improve the performance and buildup of coatings (Ref 4, 5). In this

Nomenclature

ε^*	strain rate
$\varepsilon_{\text{eff}}^{\text{p}}$	effective plastic strain
γ_0	Gruneisen γ
μ	relative volume
ρ	density
σ_{eff}	effective stress
A, B, N, C, M, D, S_1, S_2, S_3, γ_0, and a	input constant parameters
a	first-order volume correction to γ_0
C_{P}	particle heat capacity
E	internal energy per initial volume
f_j	quantity f for neighbor particle
h	distance
m_j	mass
n	number of neighbor particles
P	mean stress (pressure)
r_j	position
S_1, S_2, and S_3	the coefficients of the slope of the u_s–u_p curve
T	temperature
T_{m}	melt temperature
T_{ref}	reference temperature
W	smoothing kernels

process, numerical simulations were traditionally performed at a single scale for aggregate particles. Hansbo and Nylen (Ref 6) developed a model to simulate coating layer buildup and robot motion without considering the internal coating microstructure. The work of Barradas et al. was focused on the laser shock flyer used for the impact simulation of particle/substrate interactions in cold spray (Ref 7). The paper of Shimizu et al. concentrated on simulation of the flattening process of a high-temperature and high-speed droplet with molecular dynamics (Ref 8). Shi and Christofides focused on the computational modeling of coating microstructure produced by a high-velocity oxygen-fuel thermal spray process. In the coating growth model, the complex characteristics of coatings were captured by applying certain basic rules in the deposition process. In the microscopic particle deposition process, the formation of coating microstructure is captured by the Madejski deformation model and several rules that govern splat formation, solidification, and coating growth (Ref 9, 10).

However, the high-performance coatings fabricated with agglomerate particles are an important part of the thermal spray technique (Ref 11), and the behavior of agglomerate particles depositing on substrate is not reported. Here, the agglomerate particles should be considered as multiscale particles, such as nanoscale particle clusters (Ref 12, 13), whose deposition behavior differs from that of aggregate particles. Thus, the authors wanted to research the deposition mechanism of agglomerate particles in the thermal spraying process. Luckily, some deposition characteristics of agglomerate particles can be simulated with smoothed particle hydrodynamics (SPH) theory (Ref 14), which is a non-mesh-based computational method for simulating fluid flows, solid deformation, and coupled fluid-structure systems that may serve to characterize physical clustering of particles (Ref 15). It is particularly powerful for predicting complex free surface motion and is able to capture fine features in the contact surfaces with little numerical diffusion (Ref 16) Thus, it has been found to be well suited to modeling the deposition characteristics for thermal sprayed coatings.

In this paper, in order to discover the significant metallic bonding between the precipitates, the work employs the mesh-free SPH technique and the explicit time integration nonlinear finite element code LS-DYNC (Ref 17) to analyze how the multiscale agglomerate particles impact on the substrate in the LTHVAF spraying process. The finite element method (FEM) and SPH can be used for particle impact at the different scales, and the relationships between them are analyzed. Lastly, the buildup of the coatings with agglomerate particle is described.

2. Numerical Model

2.1 Multiscale Geometric Models

In the LTHVAF spraying process, the agglomerate particles with high velocity deposited continuously on the substrate (or previous coatings) can build the coatings up. In this paper, the model strategy is shown as:

- Research of iron (Fe) particles depositing on the substrate (or previously deposited coating) for the coating buildup should use the LS-DYNC deformation dynamic response of finite element analysis.
- The SPH geometrical model may be used for the agglomerate particle.
- The size of agglomerate particles is 20 μm.

The deposition stress of agglomerate particle can change with the time and structure deformation when impacting on the substrate. The energy of agglomerate particles that contacted previous coatings (or substrate) will affect coating performance. The model developed in this study is based on the following main assumptions:

- The geometry of multiscale particle impact is simplified to three states: continuous particles and continuous particles, agglomerate particles and continuous substrate, and agglomerate particles and agglomerate substrate. The geometrical models are listed in Table 1.
- The particle specific heat is independent of temperature.
- The agglomerate metal particle might exchange energy only with the substrate and not participate in any chemical reaction.
- The entire interface is lubricous.

The coating characteristics can be described with the impacting particles of different sizes at different axial stresses when the coatings build up step by step. The different scale geometrical models of particles impacting on substrate is shown in Fig. 1.

2.2 Johnson-Cook Constitutive Model

For the continuous particle impacting on the substrate, a purely phenomenological model is considered, which is from Johnson and Cook (Ref 18). The Johnson-Cook model is known for its simplicity and the availability of parameters for parameters for various materials of interest. It is commonly used in the simulation of highly dynamic processes. These three key material responses are strain hardening, strain-rate effects, and thermal softening; these

Table 1 Model for multiscale particle at three states

No.	Relationship between the particle and substrate	Simulated model
1	Continuous particle and continuous substrate	FEA-FEA (particle-substrate)
2	Agglomerate particle and continuous substrate	SPH-FEA
3	Agglomerate particle and disperse substrate	SPH-SPH

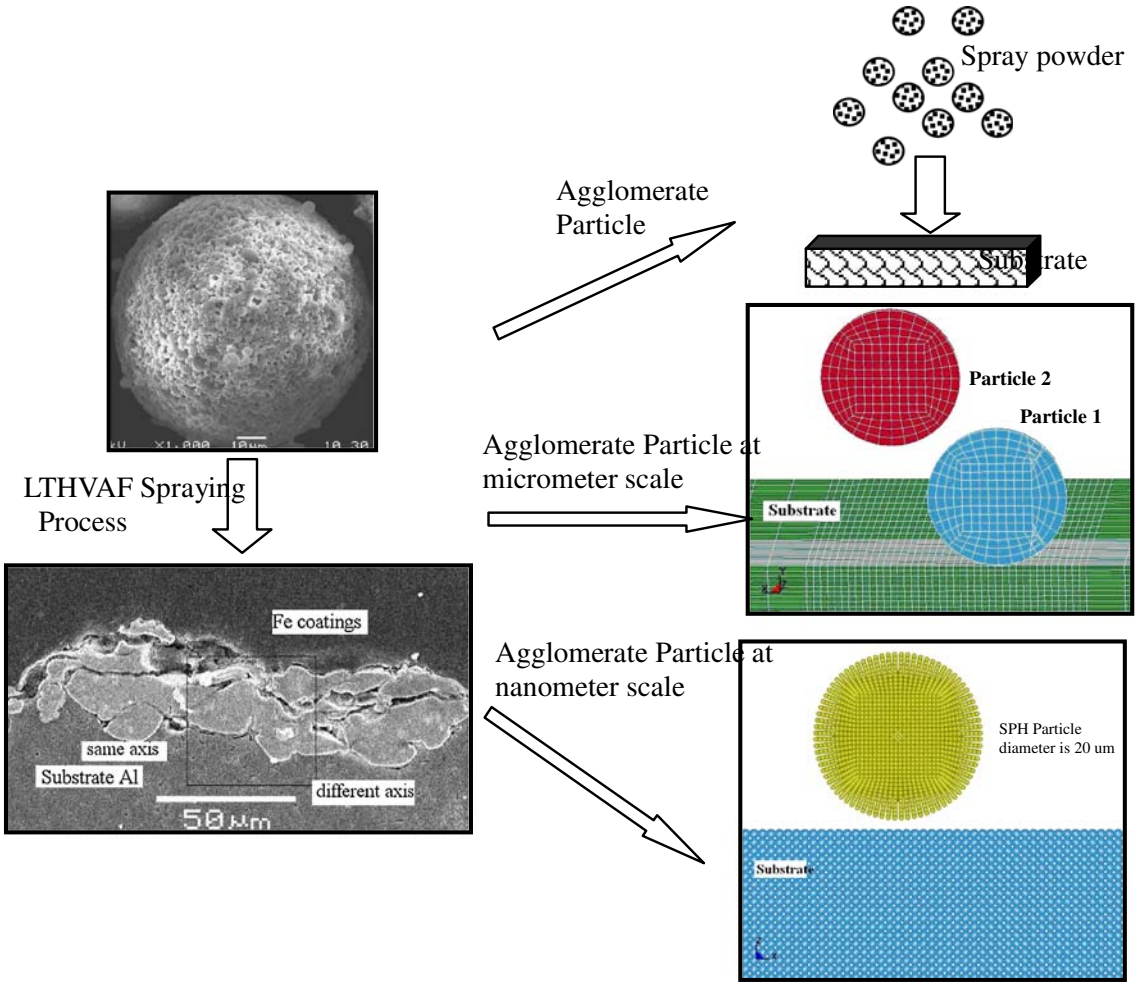

Fig. 1 Multiscale model of agglomerate particle in the low-temperature high-velocity air fuel spraying process

effects are combined, in a multiplicative manner, in the Johnson-Cook constitutive model, which is expressed as:

$$\sigma_y = (A + B\varepsilon_{\text{eff}}^{\text{p}\,N})(1 + C\ln\varepsilon^*)(1 - T^{*M}) \quad \text{(Eq 1)}$$

where the yield strength portion of the Johnson-Cook constitutive model has five parameters: A, B, N, C, and M, and three material characteristics: ρ, C_P, and T_m; $\varepsilon_{\text{eff}}^{\text{p}}$ is effective plastic strain; $\varepsilon^* = \dot{\varepsilon}_{\text{eff}}^{\text{p}}/\dot{\varepsilon}_0$ is the strain rate used to determine A, B, and N; and $T^* = (T - T_{\text{ref}})/(T_m - T_{\text{ref}})$ is the homologous temperature, where T_m is melt temperature, T_{ref} is reference temperature; $\Delta T = (1/\rho C_P)\int \delta d\varepsilon_{\text{eff}}^{\text{p}}$.

Based on cumulative plastic strain, the cumulative-damage fracture model is given by:

$$\varepsilon^{\text{f}} = \left[D_1 + D_2 \exp\left(D_3 \frac{P}{\sigma_{\text{eff}}}\right)\right][1 + D_4 \ln\varepsilon^*][1 + D_5 T^*] \quad \text{(Eq 2)}$$

where $D_1 = \sum \Delta\varepsilon_{\text{eff}}^{\text{p}}/\varepsilon^{\text{F}}$ is failure that occurs when $D = 1$, σ_{eff} is effective stress, and P is mean stress (pressure); this is similar in form to the yield strength model where the three terms combine in a multiplicative manner to include the effects of triaxial stress, strain rate, and local heating, respectively. This portion of the Johnson-Cook constitutive model requires an additional five model parameters.

Additionally, the state characteristics in the deposition process are required. Typically, the shear modulus is input along with an equation of state (EOS) used to define pressure versus volume strain response; for low pressure, the EOS is assumed to be defined by elastic bulk modulus. The Gruneisen equation of state with cubic shock velocity-particle defines pressure for compressed material as (Ref 19):

$$p = \frac{\rho_0 C^2 \mu\{1 + [1 - (\gamma_0/2)]\mu - (a/2)\mu^2\}}{\{1 - (S_1 - 1)\mu - S_2[\mu^2/(\mu + 1)] - S_3[\mu^3/(\mu + 1)]\}^2} + (\gamma_0 + a\mu)E \quad \text{(Eq 3)}$$

where E is the internal energy per initial volume, C is the intercept of the u_s-u_p curve, S_1, S_2, and S_3 are the coefficients of the slope of the u_s-u_p curve, γ_0 is the Gruneisen γ, and a is the first-order volume correction to γ_0. Constants C, S_1, S_2, S_3, γ_0, and a are all input parameters. The compression is defined in terms of the relative volume,

Table 2 Material parameters of particle and substrate

Materials	Elastic constants and density			Yield stress and strain hardening			Strain-rate hardening		Pressure cutoff (σ_m), GPa
	E, GPa	ν	ρ, kg/m^3	A, MPa	B, MPa	n	$\dot{p}_0$, $\dot{r}_0$, s^{-1}	C	
Fe (Ref 20)	207	0.3	7850	792	510	0.26	5e − 4	0.014	0.24
Ly12Al (Ref 21)	28.6	0.33	2780	369	684	0.34	6.2e − 4	0.015	1.67

	Adiabatic heating and temperature softening				Fracture strain constants				
	C_P, J/kg · K	T_m, K	T_0, K	m	D_1	D_2	D_3	D_4	D_5
1006Fe	452	1800	500	0.94	0.0705	1.732	−0.54	−0.0015	···
Ly12Al	904	775.15	300	1.7	−0.54	4.89	−3.03	0.014	1.12

Table 3 Equation-of-state (EOS) parameters of the particle and substrate

Material	C	S_1	S_2	S_3	γ_0	A	E_0	V_0
Fe (Ref 20)	0.4569	1.49	0.0	0.0	2.17	0.46	0.0	1.0
Ly12Al (Ref 22)	0.5328	1.338	0.0	0.0	2.0	0.48	0.0	

$\mu = \rho/\rho_0 - 1$. For expanded materials, the pressure is defined by:

$$p = \rho_0 C^2 \mu + (\gamma_0 + \alpha\mu)E \quad \text{(Eq 4)}$$

In this paper, the parameters of Fe material come from Ref 20, and the parameters of Ly12Al (2024Al) materials can be found in Ref 21 and in Table 2. The EOS parameters of the particle and substrate are listed in Table 3.

2.3 SPH Fundamentals

The SPH method is based on interpolation theory, in which an arbitrary field function $f(r)$ (and its derivatives) is expressed in terms of its values at a set of disordered points, which is an approximation method for the particle system. One can estimate a function f at position r by using smoothing kernels W to approximate in a local neighborhood within distance h (Ref 16, 23):

$$f(r) = \sum_{j=1}^{n} m_i \frac{f_j}{\rho_j} W(r - r_j, h) \quad \text{(Eq 5)}$$

where m_j is the mass, r_j is the position, ρ_j is the density, and f_j is the quantity f for neighbor particle j. Here, n is the number of neighbor particles with $|r - r_j| \le h$. To shorten the equation, we omit the n in all summations. When $r = r_i$, $f(r)$ is denoted by f_j.

Thus, we estimate the density ρ_i for a particle i at location r_i by

$$\rho_i = \sum_{j=1}^{n} m_i W(r - r_j, h) \quad \text{(Eq 6)}$$

where the kernel function, W, should normalize to unity and become a delta function in the limit where the characteristic smoothing length h approaches zero. The kernel function is usually chosen to be differentiable, non-negative, and symmetric, $W(r',r;h) = W(|r' - r|,h)$, where the integration is over the entire space. The choice of a kernel function with finite support is, however, essential in order to reduce the number of particle interactions and therefore code efficiency. For the subsequent discussion, the frequently used third-order B-spline function in d-dimensional space is our choice of "generic" kernel function:

$$W(r', r; h) = \frac{1}{N(\delta)h^{\delta}} \begin{cases} 1 - \frac{3}{2}q^2 + \frac{3}{4}q^3 & |q| \le 1 \\ \frac{1}{4}(2-q)^3 & 1 < |q| \le 2 \\ 0 & 2 < |q| \end{cases} \quad \text{(Eq 7)}$$

where $q = (|r' - r|/h)$ and the normalization factor $N(\delta) = \{3/2, 7/10, \pi, \pi, 31/10\ \pi^2, 3/5\ \pi^2\}$ for $\delta = 1, \ldots, 5$.

The SPH momentum equation used for the fluid flow is (Ref 14):

$$\frac{dv_a}{dt} = \mathbf{g} - \sum_b m_b \left[\left(\frac{P_b}{\rho_b^2} + \frac{P_a}{\rho_a^2} \right) - \frac{\xi}{\rho_a \rho_b} \frac{4\mu_a \mu_b}{(\mu_a + \mu_b)} \frac{v_{ab} r_{ab}}{r_{ab}^2 + \eta^2} \right] \times \nabla_a W_{ab} \quad \text{(Eq 8)}$$

where P_a and μ_a are pressure and viscosity of particle a and $v_{ab} = v_a - v_b$. Here ξ is a factor associated with the viscous term, η is a small parameter used to smooth out the singularity at $r_{ab} = 0$, and $\mathbf{g}$ is the gravity vector.

3. Simulation Process and Experiment

3.1 Information on the Simulation Process

In order to produce reasonable resolution in the simulation process, computer information on the computation process for the particle and substrate at the relevant scale, such as continuous-continuous, SPH-continuous, and SPH-SPH, is listed in Table 4.

3.2 Experiment for Coating Buildup

This experiment was designed to report the deposition behavior of the agglomerate particle in the LTHVAF spraying process. The low-temperature supersonic flame can be obtained (≥200 °C) when the parameters of the LTHVAF spraying system are:

- Fuel/air flow rate: kerosene, 2.5 L/h; O_2, 8 m^3/h; N_2, 25 m^3/h

- Powder carrier gas (N_2): 5 L/h
- Spray distance: 100 mm

The spray powder is Fe particle, and the substrate is Al, the previous deposition surface of which is polished.

Table 4 Basic computer information

Particles velocity, m/s	CPU time, s	CPU time and clock time per zone cycle, ns
Element No. of continuous particle: 2048; Element No. of continuous substrate, 72,000		
300	11,889	2,369
400	6,989	2,359
450	6,302	2,498
500	9,533	2,527
600	7,100	2,390
700	7,882	2,882
900	9,186	2,953
No. of SPH particle: 32,000; Element No. of continuous substrate: 256,000		
300	2,558	12,807
400	1,662	6,405
500	39,797	1,842,024
No. of SPH particle: 32,000; No. of SPH substrate: 256,000		
400	6,894	41,016
500	7,112	42,202
700	3,011	32,130

4. Results and Discussion

4.1 Depositing Characteristics of Agglomerate Particle at Microscale

As shown in Fig. 1, the agglomerate particle can be described with two states: continuous and SPH agglomerate unit. At the micrometer scale, the agglomerate particle can be considered a continuous unit whose depositing behavior can be simulated with FEM.

In Fig. 2, the deposition process of two particles with different axes impacting on substrate are shown; the initial velocity is 500 m/s, and the initial temperature is 500 K. The particle impacts on the substrate, the stress between the substrate and particle occurs, and they distorts synchronously. Then, a later particle impacts the previous particle and deposits on the substrate, which can induce stress turbulence at the contact interface. Next, the second particle destroys the state of first particle. Thus, during the coating buildup process, the second deposited particle can tamp the previous coatings. However, at the region where there is no impacting stress, the edge of the first deposited particle will be warped up (Ref 24). Additionally, the focus stress can occur at the extruded region for the later particles. The interface between coatings and substrate is shown to involve complex morphological and metallurgical phenomena that can be claimed to govern macroscopic properties, primarily coating-substrate adhesion. The most

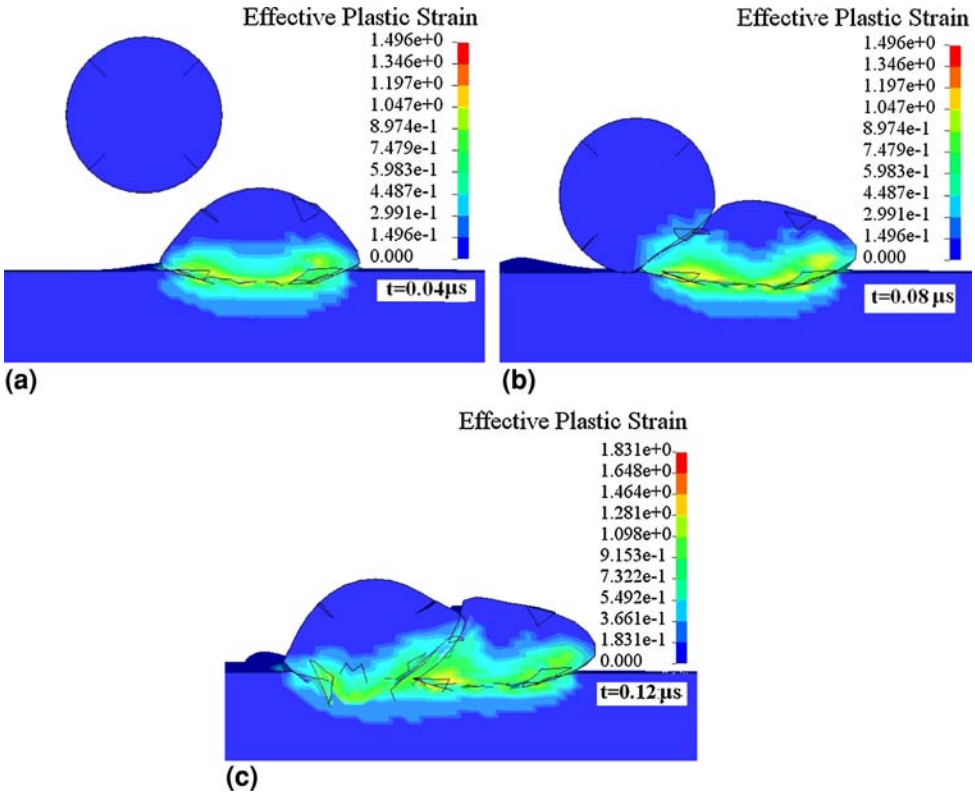

Fig. 2 Deposition characteristics of two particles at different axes ($v = 500$ m/s, $T = 500$ K)

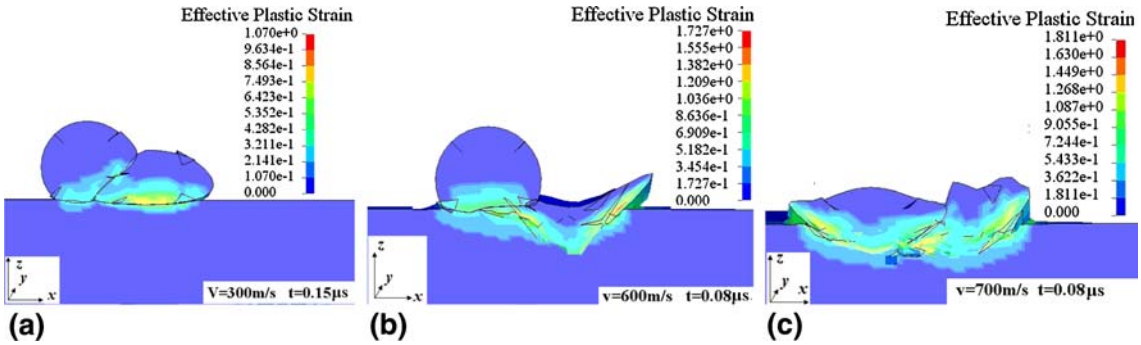

Fig. 3 Effect of the particle velocity on the plastic strain

prominent of these mechanisms was that of transient melting at the coating/substrate interface formed for the impacted particle. It is propitious to deposit thick coatings and improve the performance of coatings.

In order to research the effect of agglomerate particle velocity on coating buildup at micrometer scale, the deposition processes of particles with different velocities are shown in Fig. 3. The effective plastic strain of the particle increases with the increase of particle velocity. In contrast, the effective strain of the particle decreases when the particle velocity is 900 m/s. This indicates that the effective plastic strain can approach a certain value when the particle velocity exceeds the threshold velocity. Additionally, the compressed volume ratio of the previous particle increases insensitively when the later particle, which flattens and compresses, impacts on the previous coatings. In this process, the contacted interface can cause transient melting for the stress focus. In this way, the relationships between the coating structure and interface morphology can be established in the low-temperature HVAF spray process.

Certainly, the previous particle can be compressed at the high velocity. This can improve the coating quality, especially by decreasing the porosity. The compressed volume ratio of an agglomerate Fe particle at different velocities is shown in Fig. 4, where only the first particle is shown. When the particle impacts on the substrate, with the increase of the particle temperature and velocity, there is an increase in the particle compression ratio. There exists a threshold at 500 to 600 m/s. This shows that the instantaneous rate of change of particle volume compression ratio decreases when the particle velocity increases. Although the volume of the particle can change with the increase of velocity in the spraying process, the relationship in the particles is not compact for the low flattened ratio when the particle velocity is less than 500 m/s. This indicates that the porosity in the coatings may increase and cause a decline in the coating performance.

Figure 5 shows the temperature change in the interface between the particle and substrate when the initial size, velocity, and temperature of Fe particle are 20 μm, 500 K, and 500 m/s, respectively. Obviously, the elements (S817, S821, S7271, S7001, and S6701) come from the particle and

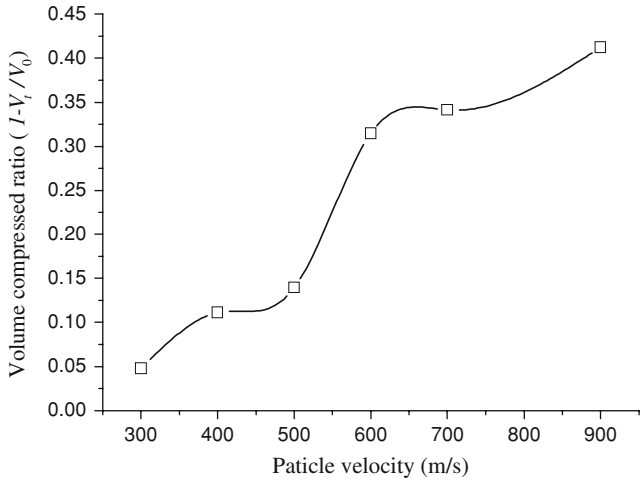

Fig. 4 Effect of the particle velocity on volume compressed ratio

the interface at the substrate surface (Fig. 5a). Figure 5(b) shows the surface temperature of particle (S817, S821), and the contacted element (S7001) increases to 600 to 630 K (0.02 μs) quickly when the particle contacts the substrate surface. Latterly, the others at the contact surface can slowly increase to 450 to 550 K. This shows that the contact surface changes continuously during the deposition process.

During the impact process, the energy exchanged between the particle and substrate exists in two models: the heat conduction and the heat energy transformed from the particle movement energy. Certainly, the movement energy is the main resource, which can cause the geometry model to change form and increase the temperature at the contacted interface. Then, the heat energy can transmit to the low plastic strain region for the heat conduction. The temperature of substrate decreases slowly. Compared with temperature of S7271, S7001, and S6701 in the substrate, the maximum temperature can occur at the S7001 element. It shows that there is an angle (about 30°) where the element exists at maximum strain and the maximum temperature changes. Here, transient melting can be ascertained in an approach to the achievement of

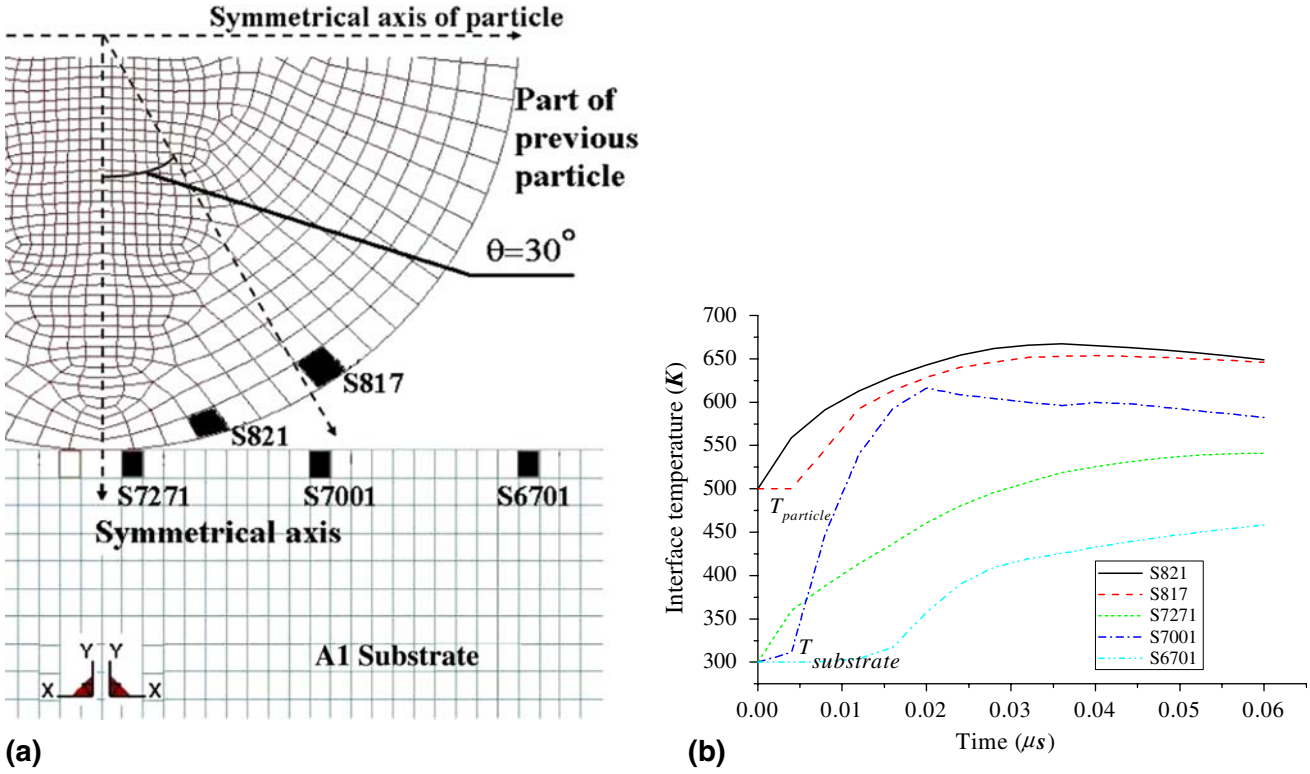

Fig. 5 Temperature change at the interface affected by the Fe agglomerate particle. (a) Grid characteristics. (b) Temperature change of the interface element

intermetallics combined with the modeling of the particle penetrating into the substrate.

4.2 Deposition Characteristics of Agglomerate Particle at Nanoscale

Sometimes, the particle impinging on the substrate can splash during the spraying process, especially for the agglomerate particles. Additionally, the diffusion region between the particle and the substrate is important to the LTHVAF sprayed coatings. It can improve the adhesive strength at the interface of the coatings and substrate. Evidently, the simulation at the simple scale for the particle deposited on the substrate cannot explain these phenomena. So, the agglomerate particles impacting on the substrate should be researched at the different scales, which can be defined with the SPH particle.

The deposition state and the effective plastic strain of agglomerate particles impacting on the substrate at 400 m/s and 500 K are shown in Fig. 6. During the flying process, the agglomerate particle can be constructed a aggregation when the adhesive in the agglomerate particle decomposes. Then, the particle clusters impacting on the substrate can be splashed at the different content for the turbulent momentum, which is shown in Fig. 6(a-c). Synchronously, the large force produced in this process can cause the obvious plastic strain at a certain region in the substrate, which can be found in the Fig. 6(d, e). This turbulent force can make the particle crack (Fig. 6f).

4.3 Interface Characteristics Between Agglomerate Particle and Substrate

In order to describe the supersonic impact phenomenon in the depositing process, the selected equation in the work can formulate the complex behaviors at high pressure and high strain rate. The equation of state can describe the melt and gasification processes. The contracting characteristics of the multiscale particle at 500 m/s are shown in Fig. 7. As can be seen, there is an interface layer between the impacted agglomerate particle and the strain region of substrate. In this region, the particle element mixed with the substrate element for the turbulent force. It indicates that the diffusion layer may appear when the particle impacts on the substrate. This can demonstrate the feasibility of reproducing metallurgical and morphological interface mechanisms involved in LTHVAF spraying process.

In order to expatiate upon this phenomenon, the effect of the particle velocity on the depositing interface characteristics is shown in the Fig. 8. When the particle velocity exceeds the critical velocity, the layer at the interface between the agglomerate particle and substrate becomes more and more obvious with the increase of the particles. Additionally, the subcounterforce can increase with high velocity; so, the apparent sparking phenomenon increases with the increase of the particle velocity.

The aforementioned conclusions featured the role of local phenomena, which suggests the actual existence of a

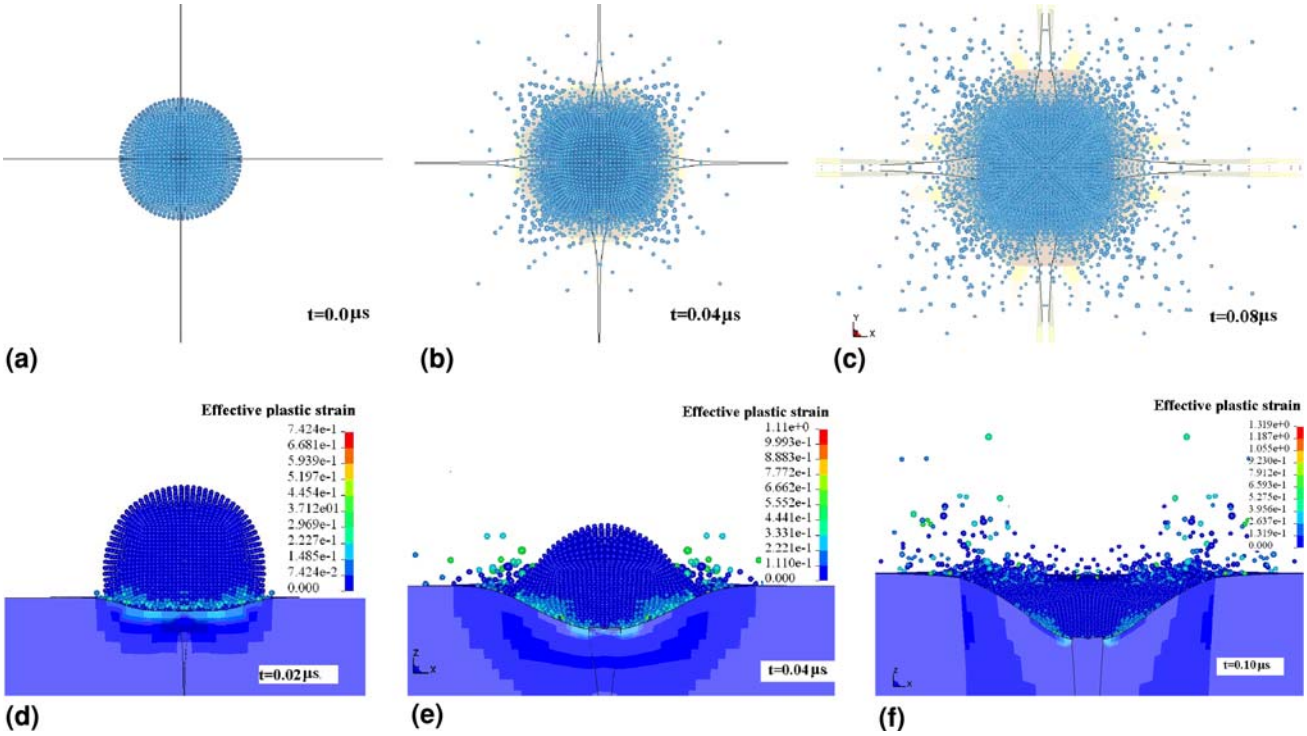

Fig. 6 Deposition state of the agglomerate particle ($v = 400$ m/s). (a), (b), and (c) Deposition state of agglomerate particle. (d), (e), and (f) Effective plastic strain of agglomerate particle

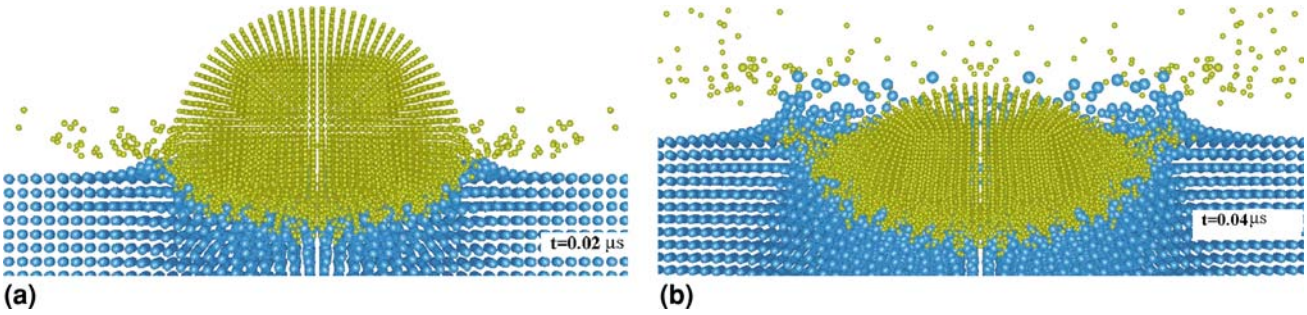

Fig. 7 Deposited interface between Fe particle and substrate

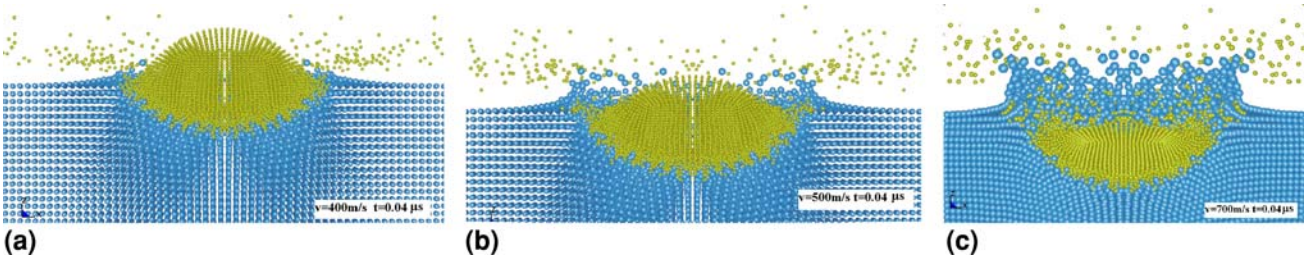

Fig. 8 Effect of the particle velocity to the depositing interface. (a) Particle velocity is 400 m/s. (b) Particle velocity is 500 m/s. (c) Particle velocity is 700 m/s

narrow window for processing conditions for some materials. This can be found in Fig. 9. As a marker for diffusion was detected through the entire interface thickness, the same transition could form layers of about 20 nm in thickness typically (Ref 7, 11). The importance of the mechanism is that of transient melting at the coating/substrate interface that formed from the impacted particle in the LTHVAF spraying process. Transient melting was

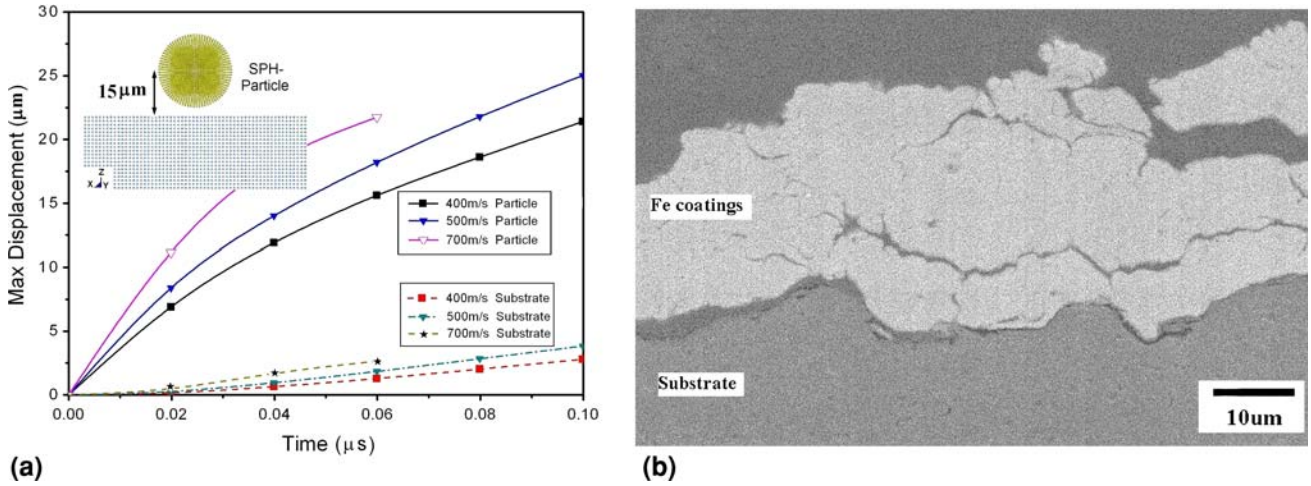

Fig. 9 The maximum displacement and interface characteristics of the depositing particle. (a) Element displacement. (b) Micromorphology of Fe coatings

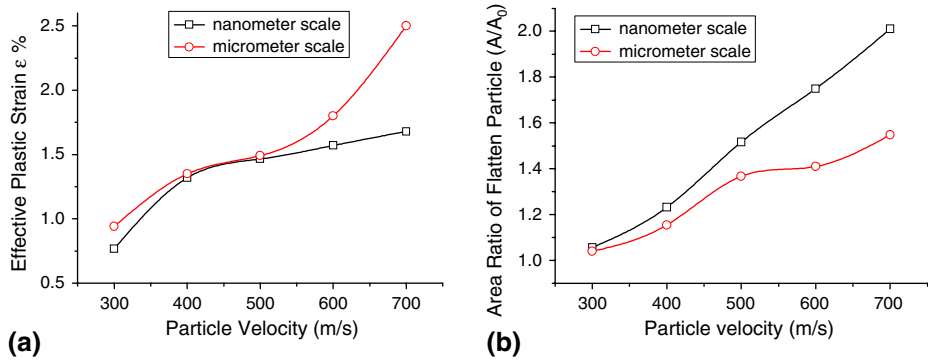

Fig. 10 Effective plastic strain and area ratio of different scale particles ($T_p = 500$ K). (a) Effective plastic strain. (b) Area ratio

ascertained by liquid-state diffusion calculations in an approach to the intermetallics combined with the modeling of the particle impinging on the substrate.

4.4 Relationship of Deposition Behavior Between Two Models

Figure 10 shows the numerical simulation of effective plastic strain and flattened area ratio when a multiscale agglomerate particle impacts on the substrate at different velocities. From the Fig. 10(a), when the particle velocity is less than critical velocity, the crack in the agglomerate particle is small, so the particle deposited on the substrate takes on the agglomerate state. Also, a small effective strain appears on the substrate. The potent proof is that the critical velocity of Fe particle is about 620 to 640 m/s (Ref 25), which can decrease when the particle temperature increases (Ref 26). This shows that the elastic strain can only exist at the interface of the particle and substrate. In contrast, the agglomerate particle can splash and crack when the particle velocity exceeds the critical velocity (Fig. 6f).

Compared with deposited state of a differently simulated model, the effective plastic strain of particle at nanoscale is less than that the microscale. This indicates that the uncompacted state of agglomerate particle can lead to the turbulent force when the particles impact on the substrate, which can reduce the penetrated performance of particle at the nanoscale. This behavior can decrease the stress-strain of substrate and cause the cracked particle to sparkle. Additionally, the agglomerate particle area ratio (A/A_0) of the flattened particle after impacting on the substrate is shown in Fig. 10(b). When the micrometer particle velocity is less than 500 m/s, the area ratio of the flattened particle increases as the velocity increase. Also, the rate of area ratio increases slowly when the particle velocity exceeds the velocity. It indicates that the contact energy between the agglomerate particle and substrate at the microscale can cause the particle to crack when the velocity is less than the critical velocity.

However, when the velocity exceeds the critical velocity, there is a linear relationship between the cracked area and the agglomerate particle velocity at the nanoscale with SPH model. The result shows that the area ratio of agglomerate flattened particle is larger than that of the other because there is little force in the agglomerate

particles. It indicates that it is difficult for the agglomerate particle to deposit on the substrate because of the turbulent force generated during the impacting process.

5. Conclusions

In this paper, the authors simulated a three-dimensional model at multiscales for an agglomerate Fe particle deposited on the substrate (or previously deposited coating) using the LTHVAF spraying process. The physical impact phenomenon of the agglomerate particle is researched. Results include:

- The temperature and velocity of particle can affect the effective temperature and plastic strain at the contact interface for increasing particle energy, and the unflattened particle is a key to restricting the bonding strength of the coating.
- During the coating buildup process, the deformation of the deposited particle results in the coarseness of the coating surface so that the Fe particle critical velocity would be decreased. The flying particle impacting on the deposited particle produces a second deformation and temperature increase of the previously deposited coatings at the microregion. The transient melting can be ascertained at an angle (about 30°) in an approach to the achievement of intermetallics combined with the modeling of the particle penetration into the substrate.
- SPH can be used to describe the deposition behaviors of particle clusters with substrate. The uncompacted state of agglomerate particle can lead to the turbulent force when the particles impacts on the substrate, which can reduce the penetration performance of particle. This behavior can decrease the stress-strain of substrate and cause the cracked particle to sparkle.

As a result, the work presented in this paper proposes the multiscale simulation of the depositing mechanism with agglomerate metal particles in the LTHVAF spraying process. Some physical features in the coatings can be explained, such as interface layer. It can become a powerful tool for improving the coating buildup with agglomerate particles in the spray process.

References

1. X. Yuan, H. Wang, G. Hou, and B. Zha, Numerical Modeling of a Low Temperature High Velocity Air Fuel Spraying Process with Injection of Liquid and Metal Particles, *J. Therm. Spray Technol.*, 2006, **15**(3), p 413-421
2. S.V. Klinkov, V.F. Kosarev, and M. Rein, Cold Spray Deposition: Significance of Particle Impact Phenomena, *Aerosp. Sci. Technol.*, 2005, **9**, p 582-591
3. B. Zha, H. Wang, and K. Xu, Microstructure and Property of LTHVOF Sprayed Copper Coatings, *Proc. ITSC2005—Thermal Spray Connects: Explore Its Surfacing Potential!* E. Lugscheider, Ed., May 2-4, 2005 (Basel, Switzerland), 2005
4. G Wei, H. Xiong, L. Zheng, and H. Zhang, An Advanced Ceramic Coating Buildup Model for Thermal Spray Processes, *Proc. ITSC2004—Thermal Spray Solutions: Advance in Technology and Application*, May 10-12, 2004 (Osaka, Japan), 2004
5. R. Dhiman and S. Chandra, *Predicting Splat Morphology in a Thermal Spray Process*, C. Moreau and B. Marple, Eds., ASM International, Materials Park, OH, 2003, p 207-213
6. A. Hansbo and P. Nylen, Models for the Simulation of Spray Deposition and Robot Motion Optimization in Thermal Spraying of Rotating Objects, *Surf. Coat. Technol.*, 1999, **122**, p 191-201
7. S. Barradas, R. Molins, and M. Jeandin, Laser Shock Flier Impact Simulation of Particle-Substrate Interactions in Cold Spray, *Proc. ITSC2005—Thermal Spray Connects: Explore Its Surfacing Potential!*, May 2-4, 2005 (Basel, Switzerland), 2005
8. J. Shimizu and E. Ohmura, Molecular Dynamics Simulation on Flattening Process of a High-Temperature and High-Speed Droplet, *Proc. ITSC2004—Thermal Spray Solutions: Advance in Technology and Application*, May 10-12, 2004 (Osaka, Japan), 2004
9. D. Shi, M. Li, and P.D. Christofides, Diamond Jet Hybrid HVOF Thermal Spray: Rule-Based Modeling of Coating Microstructure, *Ind. Eng. Chem. Res.*, 2004, **43**, p 3653-3665
10. M. Li and P.D. Christofides, Multi-scale Modeling and Analysis of an Industrial HVOF Thermal Spray Process, *Chem. Eng. Sci.*, 2005, **60**, p 3649-3669
11. H. Gao, L. Zhao, D. Zeng, and L. Gao, Molecular Dynamics Simulation of Au Nano-scale Particle Deposited on Au Surface During Cold Spraying, *Acta Metall. Sin.*, 2006, **42**(11), p 1158-1164 (in Chinese)
12. C. Berndt, Thermal Spray Processing of Nanoscale Materials, *J. Therm. Spray Technol.*, 2001, **7**(3), p 147-181
13. X. Jiang, E. Jordan, L. Shaw, and M. Gell, Deformation Behavior of Nanostructured Ceramic Deposited by Thermal Plasma Spray, *J. Mater. Sci. Technol.*, 2004, **20**(4), p 479-480
14. P.W. Cleary, M. Prakash, and J. Ha, Novel Applications of Smoothed Particle Hydrodynamics (SPH) in Metal Forming, *J. Mater. Process. Technol.*, 2006, **177**, p 41-48
15. Y. Meleán, L.D.G. Sigalotti, and A. Hasmy, On the SPH Tensile Instability in Forming Viscous Liquid Drops, *Comput. Phys. Commun.*, 2004, **157**, p 191-200
16. F. Colin, R. Egli, and F.Y. Lin, Computing a Null Divergence Velocity Field Using Smoothed Particle Hydrodynamics, *J. Comput. Phys.*, 2006, **217**, p 680-692
17. J.O. Hallquist, *LS-DYNA Theoretical Manual*, Livermore Software Technology Corporation, Livermore, CA, 1991–1998, p 17.3
18. G.R. Johnson and W.H. Cook, Fracture Characteristics of Three Metals Subjected to Various Strains, Strain Rates, Temperatures and Pressures, *Eng. Fract. Mech.*, 1985, **21**, p 31-48
19. T. Özel and E. Zeren, Finite Element Modeling of Stresses Induced by High Speed Machining with Round Edge Cutting Tools, *Proc. 2005 ASME International Mechanical Engineering Congress & Exposition*, Nov 5-11, 2005 (Orlando, FL), 2005
20. B. Banerjee, "MPM Validation: Sphere-cylinder Impact: Medium Resolution Simulations," Report No. C-SAFE-CD-IR-04-003, August 2004
21. Y.Y. Ying, T. Hua, D. Cheng da, H. Jianbo, and Ch. Da-Nian, Sound Velocity and Release Behavior of Shock-Compressed Ly12 Al, *Chin. Phys. Lett.*, 2005, **22**, p 1742-1745
22. V. Panov, "Modelling of Behaviour of Metals at High Strain Rates," Ph.D. thesis, School of Engineering, Cranfield University, 2005-2006
23. M. Omang, S. Børve, and J. Trulsen, SPH in Spherical and Cylindrical Coordinates, *J. Comput. Phys.*, 2006, **213**, p 391-412
24. D. Zhang, P.H. Shipway, and D.G. McCartney, Particle-Substrate Interactions in Cold Gas Dynamic Spraying, *Thermal Spray 2003: Advancing in the Science & Applying the Technology*, C. Moreau and B. Marple, Ed., ASM International, Materials Park, OH, 2003, p 45-52
25. A.P. Alkimov, V.F. Kosarev, and A.N. Papyrin, A Method of Cold Gas Dynamic Deposition, *Dokl. Akad. Nauk SSSR*, 1990, **315**(1), p 1062-1065
26. C. Li, W. Li, and H. Liao, Examination of the Critical Velocity for Deposition of Particles in Cold Spraying, *J. Therm. Spray Technol.*, 2006, **15**(2), p 212-222